Effects of Microwave Gating on Nuclear Spin Echoes in Dynamic Nuclear Polarization

David Guarin, Diego Carnevale, Mathieu Baudin, Philippe Pelupessy, Daniel Abergel, Geoffrey Bodenhausen

Effects of Microwave Gating on Nuclear Spin Echoes in Dynamic Nuclear Polarization

J. Phys. Chem. Lett. 2022, 13, 175–182

David Guarin,[1] Diego Carnevale,[1,*] Mathieu Baudin,[1,2] Philippe Pelupessy,[1] Daniel Abergel,[1] Geoffrey Bodenhausen[1,*]

[1] *Laboratoire des biomolécules, LBM, Département de chimie, École normale supérieure, PSL University, Sorbonne Université, CNRS, 75005 Paris, France*

[2] *Université de Paris, Laboratoire de Chimie et Biologie Pharmacologiques et Toxicologiques, CNRS UMR 8601, Université Paris Descartes, 45 rue des Saints Pères 75006 Paris France*

Corresponding authors: Diego Carnevale

Diego.Carnevale@ens.fr

Geoffrey Bodenhausen

Geoffrey.Bodenhausen@ens.fr

Abstract Dipolar or quadrupolar echoes allow one to observe undistorted powder patterns, in contrast to simple Fourier transformations of free induction decays (FIDs). In this work, the build-up of proton polarization due to dynamic nuclear polarization (DNP) is monitored by observing echoes rather than FIDs. When the microwave irradiation is interrupted during the build-up of DNP, the electrons relax back to their Boltzmann distribution at high fields (B_0 = 6.7 T) and low temperatures 1.2 < T_{sample} < 4.0 K, so that dipolar flip-flop-flip terms involving two electrons and one proton become largely ineffective as a mechanism of proton decoherence. This leads to a prolongation of the nuclear coherence lifetime $T_2'(^1H)$. The increase in $T_2'(^1H)$ leads to transient *surges* of the amplitudes of spin echoes. Conversely, transient *slumps* of spin echoes are observed when the microwave irradiation is switched back on, due to a shortening of nuclear coherence lifetimes.

TOC Graphic

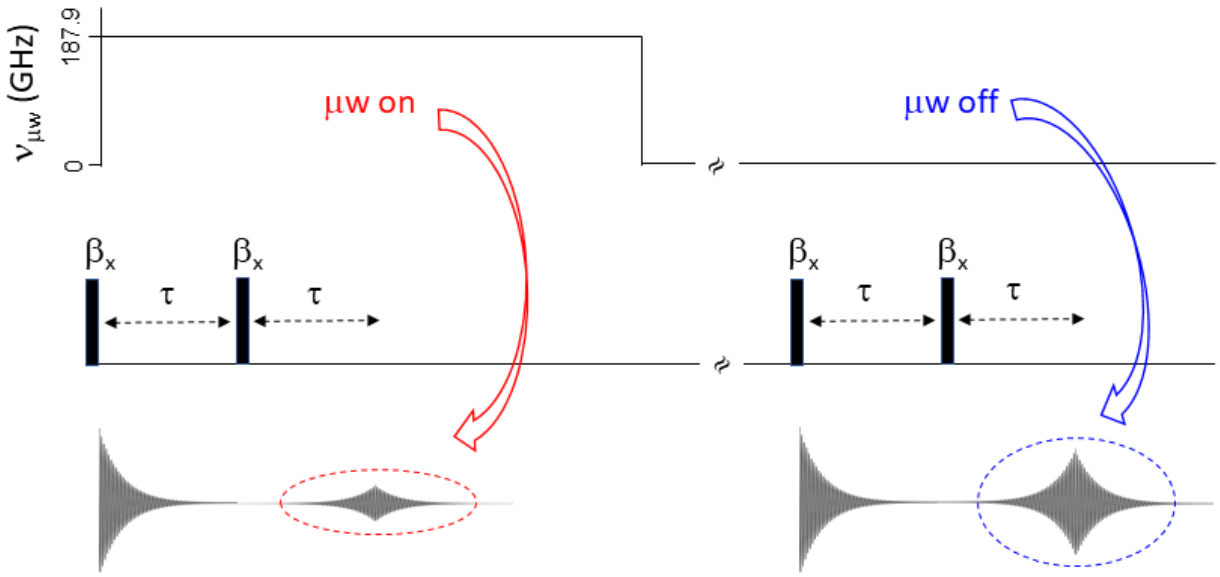

Key words

Dynamic Nuclear Polarization. Dipolar echoes. Quadrupolar echoes. Microwave gating. Transverse relaxation. Surge of spin echoes. Slump of spin echoes. Electron spin relaxation.

Dynamic nuclear polarization[1] (DNP) allows one to enhance NMR signals by several orders of magnitude.[2] This results from partial saturation of the EPR transitions of suitable radicals by microwave irradiation at low temperatures in high magnetic fields, which leads to an augmented population difference across the nuclear transitions of protons and other nuclear spins. The build-up of the nuclear polarization by DNP is usually monitored by observing free induction decays (FIDs) excited by radio-frequency (rf) pulses with small nutation angles β to preserve the hyperpolarization. However, because of unavoidable delays between excitation and signal acquisition, the Fourier transformations of FIDs do not faithfully represent broad spectra of glassy frozen solutions. To retrieve undistorted powder patterns, the observation of dipolar or quadrupolar echoes is essential. Because such echoes are attenuated by decoherence or transverse relaxation in de- and re-focusing intervals, they reveal unexpected transient variations in signal intensity.

The build-up and decay of proton magnetization in DNP experiments was monitored by means of a β- τ_{echo} - β- τ_{echo} pulse sequence to excite dipolar spin echoes using two small-angle rf pulses β = 9°. The Fourier transformations of the decaying halves of the echoes yield undistorted powder spectra.[3] The transverse relaxation during the τ_{echo} delays was found to be roughly mono-exponential at temperatures 1.2 < T < 4 K, thus justifying a phenomenological description of the decay of the dipolar echoes with an envelope $\exp\{-2\tau_{echo}/T_2'\}$ described by a 'non-refocusable' transverse relaxation or decoherence time $T_2'(^1H)$ in the laboratory frame.

At similar temperatures and in the same static field, Bornet et al.[4] have shown that the lifetime ($T_{1\rho}$) of transverse nuclear magnetization that is spin-locked in the rotating frame can be prolonged when microwave irradiation is interrupted. In this work, we report an analogous prolongation of the coherence lifetime (T_2') of transverse magnetization in the laboratory frame, determined by using dipolar echoes without spin-locking.

Each pulse with a nutation angle β = 9° leaves a fraction cos β = 0.988 of the polarization intact. When β = 9° is used as a refocusing pulse (instead of 90° as in the usual dipolar echo experiments), only a small fraction ($\sin^2 \beta$ = 0.0245) of bilinear terms such as $2I_xS_z$ and $2I_zS_x$ are interconverted. If decoherence can be neglected, the dipolar echoes are therefore weaker than

the initial FIDs by a factor of about 40, in contrast to the usual dipolar echo experiments where, neglecting decoherence, echoes and FIDs have equal amplitudes, since $\sin^2 \beta = 1$.

The receiver was activated immediately after the second pulse to observe the free induction decay (FID) excited by this pulse, which has a very similar amplitude as the FID excited by the first pulse, apart from slight phase anomalies and a negligible attenuation proportional to $\cos \beta = 0.988$. The receiver was allowed to run continuously until the echo had decayed completely. One can choose to restrict the observation to the FIDs or to the echoes.

Build-up experiments with different de- and re-focusing times τ_{echo} obtained in the absence or presence of microwave irradiation yield different transverse relaxation times $T_2'(^1H)^{(\mu W\ off)}$ and $T_2'(^1H)^{(\mu W\ on)}$. When the microwaves are switched off, the proton coherence lifetime increases by a factor

$$\kappa = T_2'^{(\mu W\ off)}/T_2'^{(\mu W\ on)}, \quad (1)$$

as was found in several samples (Table I) with compositions that are typical for dissolution DNP experiments. As can be appreciated in Fig. 1b, the echo intensity is boosted by a factor ε after the microwaves are switched off:

$$\varepsilon = \exp\{-2\tau_{echo}/T_2'^{(\mu W\ off)}\}/\exp\{-2\tau_{echo}/T_2'^{(\mu W\ on)}\}. \quad (2)$$

Hence, the ratio of the echo amplitudes to the FIDs increases, since the latter are not affected my microwave switching. A *surge* in the amplitude of the echoes is observed. Conversely, a *slump* is seen when microwaves are tuned back on. We experimentally observed surges and slumps that span time scales ranging from a few seconds to a few minutes in five different samples (Table I) at 1.2 or 4.0 K in a field $B_0 = 6.7$ T.

Table I Samples used for DNP experiments in this study.

Sample	Composition (percentages by volume)	Tempol [mM]	T_{sample} [K]	Observable proton signals	Fig.
I	glycerol-d_8/D_2O/H_2O (80/10/10)	15	1.2	H_2O, HDO	1
II	glycerol-d_8/D_2O/H_2O (50/40/10)	40	4	H_2O, HDO	2
III	DMSO-d_6/D_2O (90/10)	15	1.2	Residual protons in incompletely deuterated CHD_2SOCD_3 and HDO	3a
IV	tetrachloroethane-d_2/$CHCl_3$ (95/5)	35	1.2	$CHCl_3$	3b
V	tetrachloroethane-d_2	35	1.2	Residual protons in ca. 1% incompletely deuterated $CHCl_2CDCl_2$ in a matrix of $CDCl_2CDCl_2$	4a&b

Figure 1a shows the build-up and decay curves of FIDs (blue data points) and echoes (red data points) in sample **I,** recorded with τ_{echo} = 200 μs. Figure 1b shows FIDs and echoes before and after switching the microwave irradiation on or off. The FIDs in Fig. 1b are not affected by microwave switching, while the magnitude of the weak negative echoes increases when the microwave irradiation is turned off. This is highlighted in Fig. 1c, where the signals of Fig. 1b were expanded vertically. After interrupting the microwave irradiation (top panel), one observes as expected a slow decrease of the FID signals over time, reflecting the decay of the polarization $P(^1\mathrm{H})$. Note that the rate of this decay is much slower compared to the initial build up. On the other hand, the echoes show a sudden surge after switching off the microwave irradiation. The surge results from an increase in $T_2'(^1\mathrm{H})$ upon interruption of the microwave irradiation ($\kappa > 1$). Thus, unlike the FIDs, the echoes are *not* simply proportional to the proton polarization. Note that, after interrupting the microwave irradiation, the echoes decay faster than the FIDs. We shall see below that this may be attributed to proton-proton dipolar interactions.

Figure 2a shows the intensities of dipolar echoes observed for different intervals 143 < τ_{echo} < 333 μs in sample **II** during the build-up of the nuclear polarization $P(^1\mathrm{H})$ under

microwave irradiation, and during its decay after the microwave source is switched off. To reduce the experimental time and helium consumption, sample **II** was prepared with a higher radical concentration of 40 mM and investigated at a higher temperature T_{sample} = 4.0 K. At a chosen interval *t* after the beginning or the end of microwave irradiation, one can determine $T_2'(^1H)$ by fitting the decays of the echo intensities to a mono-exponential function $\exp\{-\tau_{echo}/T_2'(^1H)\}$, as shown in Fig. 2b for *t* = 12 min after switching off the microwave source, when the echoes have a low signal-to-noise ratio. The red data points in Fig. 2c show the $T_2(^1H)$ values obtained in the course of the entire build-up and decay. A marked increase in transverse relaxation time is observed when the microwave irradiation is interrupted, with $T_2'^{(\mu W\ off)}$ = 105 μs and $T_2'^{(\mu W\ on)}$ = 75 μs, and hence $\kappa = T_2'^{(\mu W\ off)}/T_2'^{(\mu W\ on)}$ = 1.4 at T_{sample} = 4.0 K. This ratio is expected to be higher at 1.2 K. Remarkably, the $T_2'(^1H)$ values are not constant, neither during the build-up nor during the decay of the polarization. The measured $T_2'(^1H)$ increase in the first three minutes of the microwave irradiation, and fall back after the surge close to their initial value about 12 min after the interruption of the microwave irradiation. These observations suggest that the electron polarization is not the only factor that determines the time-dependence of $T_2'(^1H)$ during the build-up and decay, and that nuclear polarization also plays a role. Since the nuclear polarization decreases after the microwaves are switched off, while the electron polarization increases, they have opposite effects. The gradual reduction of $T_2'(^1H)$ after the surge in Fig. 2c explains the difference between the decays of the echoes and of the FIDs observed in Fig. 1a.

A similar prolongation of $T_2'(^1H)$ has also been observed for samples **III** and **IV**, as shown in Figures 3a and 3b, respectively, both recorded at T_{sample} = 1.2 K. In Fig. 3b, the effects of microwave irradiation of the high-frequency lobe of the EPR spectrum (which leads to a negative proton polarization) has been investigated. The negative DNP effect appears exacerbated by a negative surge, again resulting from a prolongation of the lifetime $T_2'(^1H)$.

The proton concentration was further reduced by using nominally perdeuterated tetrachloroethane-d_2 (sample **V**), and by recording echoes of the residual protons ($CHDCD_2Cl_2$ has an estimated concentration below 1%.) Blue data points in Fig. 4a show experiments that

start by applying microwave irradiation to the low-frequency lobe of the EPR spectrum. The red data points refer to microwave irradiation on the high-frequency lobe of the EPR spectrum, leading to a negative enhancement. At times indicated in the diagram on top of Fig. 4a, the microwave irradiation was turned off. The transient surges of the proton echoes begin immediately after turning off the microwave irradiation.

The grey data points in Fig. 4a relate to an experiment where the microwaves were not turned off, but where the microwave carrier frequency was moved far off-resonance, well outside the broad EPR spectrum. This experiment was conducted to exclude effects due to cooling of the sample after switching off the microwave irradiation.

Figure 4b shows analogous build-up curves for sample **V** when the microwaves were turned on and off at different times within the same experimental run (red data points). For comparison, the blue data points are reproduced from Fig. 4a. Transient surges are observed at arbitrary times along the build-up curve whenever the microwaves are turned off. Slumps due to the shortening of coherence lifetimes are observed whenever the microwaves are turned on again. Under continuous microwave irradiation, the same level of polarization is eventually achieved as in conventional build-up experiments, as shown by the red data points that asymptotically approach a dynamic equilibrium represented by the dashed blue line. Surges and slumps are highlighted in Fig. 4b by blue and orange rectangles, respectively.

In sample **V**, which has a low proton concentration, the surges and slumps are much slower than was observed in other samples. The initial slopes of the surges in sample **V** can be estimated to be ca. 0.03 s^{-1}, which is much slower than $1/T_1^e \approx 20\ s^{-1}$ determined by Bornet et al.[4]

To summarize our empirical observations, surges and slumps of dipolar proton echoes have been observed in a variety of frozen solutions that are typically used for dissolution DNP, including pure solvents, both polar and apolar, with TEMPOL concentrations ranging from 15 to 40 mM, on time scales up to several minutes. Effects of microwave irradiation on the sample

temperature have been ruled out as a possible cause since moving the microwave carrier far off-resonance has the same effect as switching off the microwaves.

The experimental evidence can be rationalized in part by considering the effect of the electron polarization P_e on the transverse relaxation rate $1/T_2'(^1H)$ of the protons in the laboratory frame. In the absence of microwave irradiation at high field and low temperatures (except for Fig. 2 where T_{sample} = 4.0 K, this work used B_0 = 6.7 T and T_{sample} = 1.2 K), almost all electron spins are in their ground state ($P_e^{\alpha} \approx 1$, $P_e^{\beta} \approx 0$), so that the electron polarisation, i.e., the difference of the populations, is $P_e = P_e^{\alpha} - P_e^{\beta} \approx 1$. Indeed, as summarized by Cox et al.,[5] if a three-spin flip-flop-flip transition involves one nuclear and two electronic spins, the rate of the process is proportional to the probability that one electron of the pair is 'up' and the other 'down'. The product $P_e^{\alpha} P_e^{\beta}$ of the populations of the 'up' and 'down' manifolds can be readily expressed as a function of the electron polarization P_e: since $P_e^{\alpha} = ½ (1 + P_e)$ and $P_e^{\beta} = ½ (1 - P_e)$, one readily obtains

$$P_e^{\alpha} P_e^{\beta} = ½(1 + P_e)\, ½(1 - P_e) = ¼ (1 - P_e^2). \quad (3)$$

The factor $(1 - P_e^2)$ describes the role of the electron polarization in the three-spin flip-flop-flip process and is a characteristic signature of the "cross effect" and of "thermal mixing".[1,5] In the absence of microwaves, the flip-flop-flip terms are ineffective so that $T_2'(^1H)^{(\mu W\ off)} > T_2'(^1H)^{(\mu W\ on)}$. On the other hand, if the microwave field is sufficiently strong to saturate the electron spins, by overriding their tendency to fall back to their ground state through electron spin-lattice relaxation, one can in principle achieve $P_e^{\alpha} \approx P_e^{\beta} \approx ½$, thus allowing the electron-electron-nuclear flip-flop-flip terms to become effective. In this (unrealistic) limit, $[1-(P_e^{\mu W\ on})^2] \approx 1$. Bornet et al.[4] estimated $P_e^{\mu W\ on} \approx 0.48$ under conditions similar to ours, hence $[1 - (P_e^{\mu W\ on})^2] \approx 0.77$. When the microwave field is switched off, bearing in mind that T_{sample} = 1.2 K and B_0 = 6.7 T, we expect $[1 - (P_e^{\mu W\ off})^2] \approx 0.002$, i.e., a factor 385 smaller than $[1 - (P_e^{\mu W\ on})^2] \approx 0.77$. For T_{sample} = 4 K as used in Fig. 2, one obtains $[1 - (P_e^{\mu W\ off})^2] \approx 0.34$, i.e., still a factor 2.2 smaller than $[1 - (P_e^{\mu W\ on})^2] \approx 0.75$. Note the dramatic effects of changing T_{sample} from 4 to 1.2 K.

Switching the microwave irradiation on and off can have remarkable consequences on nuclear relaxation, as demonstrated by Bornet et al.[4] for $T_{1\rho}$ relaxation of ^{1}H nuclei in the rotating frame. Their study was carried out using similar equipment as ours, on a frozen glassy sample at 1.2 K of H_2O / D_2O / glycerol-d_8 (10 / 40 / 50% by volume) doped with 40 mM Tempol, containing (unlike our samples) 3 M [1-^{13}C] acetate. Bornet et al.[4] found that $T_{1\rho}(^{1}H)$ jumped from 10 to 200 ms after switching off the microwave field, i.e., that the rate $1/T_{1\rho}(^{1}H)$ slowed down by a factor of 20 from 100 to 5 s^{-1}. They assumed that $T_{1\rho}(^{13}C)$ would also be prolonged. As a result, the efficiency of cross-polarization from ^{1}H to ^{13}C could be boosted.

In principle, the initial slopes of the surges in our experiments provide an indirect measure of the electron relaxation rate $1/T_1^{e}$.[6–8] By estimating various parameters relating to the 'diffusion barrier' that acts as a bottleneck which slows down the diffusion of polarization between the protons close to the radicals and those in the bulk of the sample, Bornet et al.[4] estimated an electron spin-lattice relaxation time T_1^{e} = 48 ± 1 ms. To come to this conclusion, they estimated the radius of the diffusion barrier b = 1 nm, the bulk diffusion constant D = 10 nm^2s^{-1}, the non-paramagnetic leakage relaxation rate β = –8.6 s^{-1}, and the correlation time of the fluctuations of the electron dipolar field τ = 2.7690 x 10^{-4} s. Furthermore, Bornet et al.[4] realized that the EPR saturation was not complete in their experiments, since the effects of microwave irradiation are partly countered by electron spin-lattice relaxation. The partly saturated electron polarization, treated as an adjustable temperature-dependent parameter, was estimated to be $P_e^{\mu W\ on}$ = 48% at 1.2 K with a microwave power of 85 mW in an apparatus similar to ours. Considering the number of parameters that need to be estimated, we shall not attempt to determine the electron relaxation time T_1^{e} in this study.

The contributions of the proton-proton dipolar interactions to $1/T_2'(^{1}H)$ follow a trend that is opposite to the contributions of the electron bath. At very low proton spin temperatures, it seems that the dynamic broadening due to proton-proton flip-flop transitions is reduced. The contributions of the proton-proton dipolar interactions to the rate $1/T_2'(^{1}H)$ therefore become less effective as the nuclear polarization builds up under microwave irradiation. Conversely, they become more effective upon switching off the microwave irradiation, since the nuclei relax

back to their Boltzmann populations dictated by the sample temperature. This explains the different slopes of the return to thermal equilibrium of the blue and red curves in Fig. 1a.

In conclusion, we reported experimental observations of the prolongation of the nuclear coherence lifetime $T_2'(^1H)$ when microwave irradiation is interrupted during the build-up or decay of DNP. This leads to transient 'surges' of the amplitudes of dipolar echoes. In contrast, the corresponding shortening of transverse relaxation times $T_2'(^1H)$ obtained when microwaves are switched on again leads to 'slumps' of echo amplitudes. The experimental evidence is rationalized by considering that dipolar flip-flop-flip terms involving two electrons and one proton become largely ineffective when the electrons relax back to their ground state.

The Fourier transforms of the dipolar echoes of samples **I - V** only yielded featureless broad signals that do not significantly differ from the Fourier transforms of the FIDs. In experiments that we carried out on systems with isolated pairs of protons like in gypsum[3] and barium perchlorate monohydrate,[9–11] we have indeed observed a Pake-like fine structure, as shown in the Supporting Information.

All experiments were conducted in a Bruker prototype polarizer in a static field B_0 = 6.7 T (proton Larmor frequency $\nu_0(^1H)$ = 285.3 MHz) with a broadband double resonance D-DNP probe, although only ^1H signals were observed in this work. Microwave frequency modulation[12] was implemented by using a saw-tooth waveform with a rate of 1 kHz to cover a bandwidth of 200 MHz to saturate either the positive or negative lobe of the EPR spectrum. The microwaves were provided by an ELVA1 source coupled to a Virginia Diodes (VDI) frequency doubler. To obtain a positive polarization, the central microwave frequency was set to 187.9 GHz. For negative polarization, the central frequency was set to 188.38 GHz while the other parameters were kept constant.

The *rf*-field amplitude of the proton pulses was ν_1 = 25 kHz, corresponding to a nominal nutation angle $\beta \approx 9°$ for a pulse length τ_p = 1 μs. The build-up curves were monitored at intervals of 10 or 30 s by observing dipolar echoes excited by β - τ_{echo} - β - τ_{echo} - sequences using two pulses with $\beta \approx 9°$, with typical de- and refocusing intervals τ_{echo} = 100 μs, unless specified

otherwise, as in Fig. 2a. Note that the phases of the two pulses were not in quadrature, as normally required for dipolar or quadrupolar echoes. No phase-cycle was applied since the polarization and hence the echo amplitudes vary from scan to scan. Although complete refocusing of both linear and quadratic interactions cannot be achieved by such echoes, they nonetheless remove deleterious background signals and acoustic ringing of the probe. It has been shown that such echoes do not affect the microwave-driven build-up of the hyperpolarization.[13] A saturating train of 100 proton pulses with τ_p = 4 μs (β = 36°) spaced by 100 μs was applied prior to all experiments. To a good approximation, the effect of a pair of 9° pulses on the polarization can be neglected: two closely spaced pulses with β = 9° merely attenuate the polarization by a factor $\cos^2\beta$ = 0.975. The build-up profiles presented in this work were acquired with a number N of echoes that varied between 100 < N < 400, at intervals of typically 30 s, to follow the build-up and decay curves over a range of 5 to 50 min. The total attenuation can no longer be neglected for N = 100, since $\cos^{200}\beta$ = 0.084, i.e., up to 91.6 % of the polarization will be dissipated by *rf* pulses, neglecting relaxation. These losses may seem to accelerate the apparent $T_1(^1H)$ relaxation. In our experiments, the decays are slower, which suggests that the true nutation angles are smaller than the nominal β = 9°.

In contrast to Fourier transforms of FIDs, spin echoes lead to undistorted Pake patterns that can be analyzed to extract structural information encoded in the dipolar or quadrupolar couplings. Asymmetries of such Pake patterns due to violations of the high-temperature approximation allow one to accurately determine the spin temperature and hence the absolute polarization of the observed nuclei, as has been illustrated recently for deuterium echoes.[13]

The receiver was activated immediately after the second pulse to observe the free induction decay (FID) excited by this pulse and ran continuously until the echo had decayed completely. The signals were sampled at intervals of 0.25 μs, corresponding to a spectral width of 2 MHz. A dead time of 10 μs must be taken into account for the FIDs. For the echoes, this dead time was compensated for by reducing the second τ_{echo} interval empirically. The linewidths were not affected by microwave irradiation.

Supporting Information Hyperpolarized ^{1}H dipolar echoes for barium chlorate monohydrate $Ba(ClO_3)_2 \cdot H_2O$.

Dedication This paper is dedicated to the memory of our colleague Konstantin ("Kostya") L'vovich Ivanov (Siberian Branch of the Russian Academy of Sciences, Novosibirsk.) He was one of the most accomplished scientists in our field.

Acknowledgements We are indebted to Dr Maurice Goldman (Académie des sciences, Paris) for elaborate but unsuccessful attempts to rationalize the surges in terms of hypothetical hidden reservoirs of polarization, and for his lucid comment that "the surge effect was merely an artefact of the way you measure the polarization". We gratefully acknowledge Bruker Inc. for the loan of a prototype 6.7 T polarizer. This work was supported by the CNRS, the French "Equipements d'Excellence" grant "Paris en Resonance", contract ANR-10-EQPX-09, the European Research Council (ERC) for the Advanced grant "Dilute Para-Water" (agreement number 339754), and the ERC Synergy grant "Highly Informative Drug Screening by Overcoming NMR Restrictions" (HISCORE, grant agreement number 951459.)

References

(1) Abragam, A.; Goldman, M. Principles of Dynamic Nuclear Polarisation. *Reports Prog. Phys.* **1978**, *41* (3), 395–467.

(2) Ardenkjaer-Larsen, J. H.; Fridlund, B.; Gram, A.; Hansson, G.; Hansson, L.; Lerche, M. H.; Servin, R.; Thaning, M.; Golman, K. Increase in Signal-to-Noise Ratio of > 10,000 Times in Liquid-State NMR. *Proc. Natl. Acad. Sci.* **2003**, *100* (18), 10158–10163.

(3) Pake, G. E. Nuclear Resonance Absorption in Hydrated Crystals: Fine Structure of the Proton Line. *J. Chem. Phys.* **1948**, *16* (4), 327–336.

(4) Bornet, A.; Pinon, A.; Jhajharia, A.; Baudin, M.; Ji, X.; Emsley, L.; Bodenhausen, G.; Ardenkjaer-Larsen, J. H.; Jannin, S. Microwave-Gated Dynamic Nuclear Polarization. *Phys. Chem. Chem. Phys.* **2016**, *18* (44), 30530–30535.

(5) Cox, S. F. J.; Bouffard, V.; Goldman, M. The Coupling of Two Nuclear Zeeman Reservoirs by the Electronic Spin-Spin Reservoir. *J. Phys. C Solid State Phys.* **1973**, *6* (5), L100–L103.

(6) Macholl, S.; Jóhannesson, H.; Ardenkjaer-Larsen, J. H. Trityl Biradicals and 13C Dynamic Nuclear Polarization. *Phys. Chem. Chem. Phys.* **2010**, *12* (22), 5804–5817.

(7) Jóhannesson, H.; Macholl, S.; Ardenkjaer-Larsen, J. H. Dynamic Nuclear Polarization of [1-13C]Pyruvic Acid at 4.6 Tesla. *J. Magn. Reson.* **2009**, *197* (2), 167–175.

(8) Granwehr, J.; Köckenberger, W. Multidimensional Low-Power Pulse EPR under DNP Conditions. *Appl. Magn. Reson.* **2008**, *34* (3), 355–378.

(9) Long, J. R.; Ebelhäuser, R.; Griffin, R. G. ^{2}H NMR Line Shapes and Spin−Lattice Relaxation in $Ba(ClO_3)_2 \cdot {}^{2}H_2O$. *J. Phys. Chem. A* **1997**, *101* (6), 988–994.
(10) Carnevale, D.; Ashbrook, S. E.; Bodenhausen, G. Solid-State NMR Measurements and DFT Calculations of the Magnetic Shielding Tensors of Protons of Water Trapped in Barium Chlorate Monohydrate. *RSC Adv.* **2014**, *4* (99), 56248–56258.
(11) Carnevale, D.; Marhabaie, S.; Pelupessy, P.; Bodenhausen, G. Orientation-Dependent Proton Relaxation of Water Molecules Trapped in Solids: Crystallites with Long-Lived Magnetization. *J. Phys. Chem. A* **2019**, *123* (45), 9763–9769.
(12) Bornet, A.; Milani, J.; Vuichoud, B.; Perez Linde, A. J.; Bodenhausen, G.; Jannin, S. Microwave Frequency Modulation to Enhance Dissolution Dynamic Nuclear Polarization. *Chem. Phys. Lett.* **2014**, *602*, 63–67.
(13) Aghelnejad, B.; Marhabaie, S.; Baudin, M.; Bodenhausen, G.; Carnevale, D. Spin Thermometry: A Straightforward Measure of Millikelvin Deuterium Spin Temperatures Achieved by Dynamic Nuclear Polarization. *J. Phys. Chem. Lett.* **2020**, *11* (9), 3219–3225.

Figures and captions

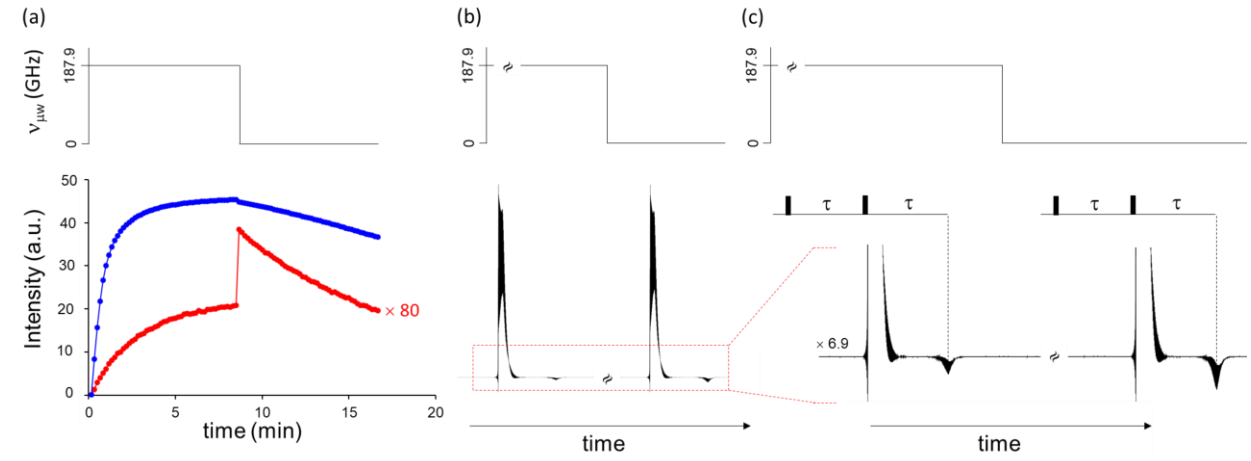

Figure 1 **(a)** Build-up of proton signals in DNP experiments performed on sample **I** at T_{sample} = 1.2 K in a static field B = 6.7 T. Single-scan dipolar echoes were excited by β_ϕ - τ_{echo} - β_ϕ - τ_{echo} - sequences with β = 9°, τ_{echo} = 200 µs and ϕ = 0°. Blue data points refer to free induction signals acquired immediately after the second pulse, whereas red data points refer to signals acquired starting on the tops of the echoes. The top panel indicates when the microwave irradiation was switched off. **(b)** Proton signals recorded before and after the microwave irradiation was switched off. The initial strong signals are FIDs, the much weaker signals with opposite phase that appear after the second τ delay are dipolar echoes. The FIDs are not significantly affected when the microwaves are switched off. **(c)** Vertical expansion showing that the dipolar echoes are more intense when the microwaves are switched off.

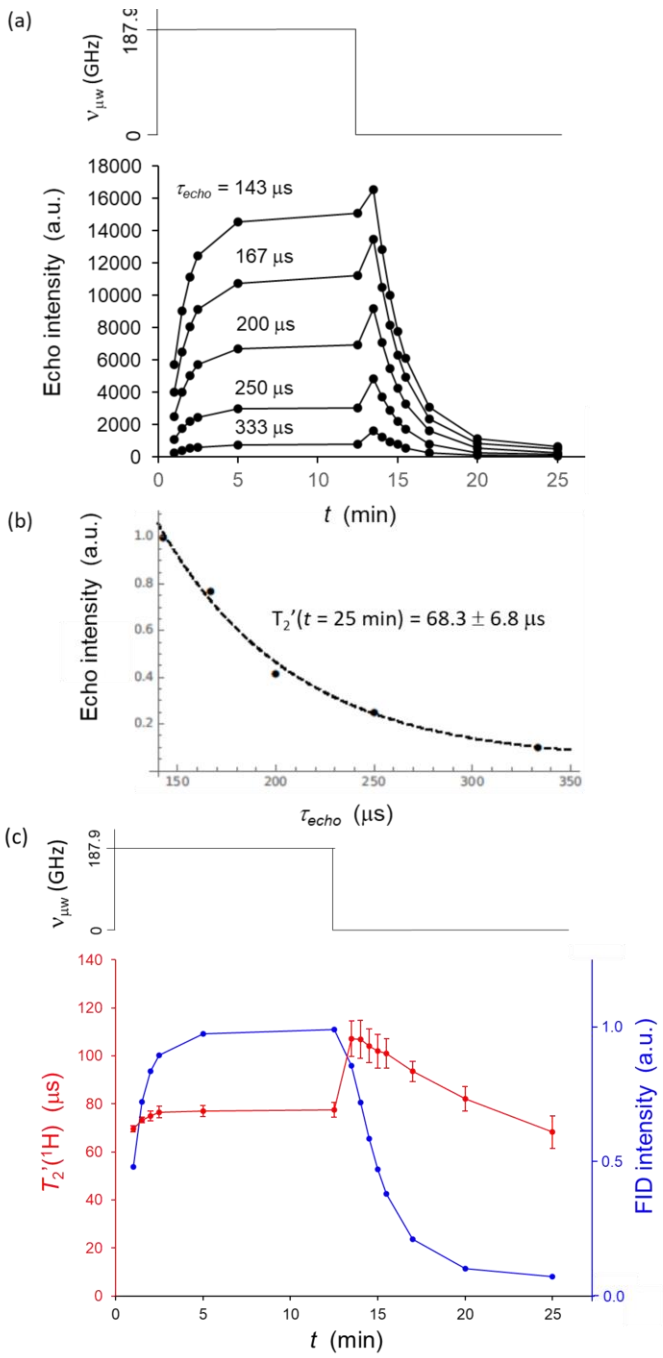

Figure 2 **(a)** Build-up curves of dipolar proton echoes of sample **II** at T_{sample} = 4.0 K, acquired with single-scan echo sequences for five intervals 143 ≤ τ_{echo} ≤ 333 µs. The top panel indicates the timing of the microwave irradiation. **(b)** Exponential decay of the dipolar proton echoes for the five experiments of Fig. 2a for *t* = 25 min. **(c)** Build-up curve (blue dots) of the FIDs observed immediately after the second pulse, ignoring the echoes. Red dots: $T_2'(^1H)$ values as a function of *t*. The error bars are given by the standard errors produced by the 'NonlinearModelFit' function as implemented in *Mathematica* 11.0. The top panel indicates the timing of the microwave irradiation.

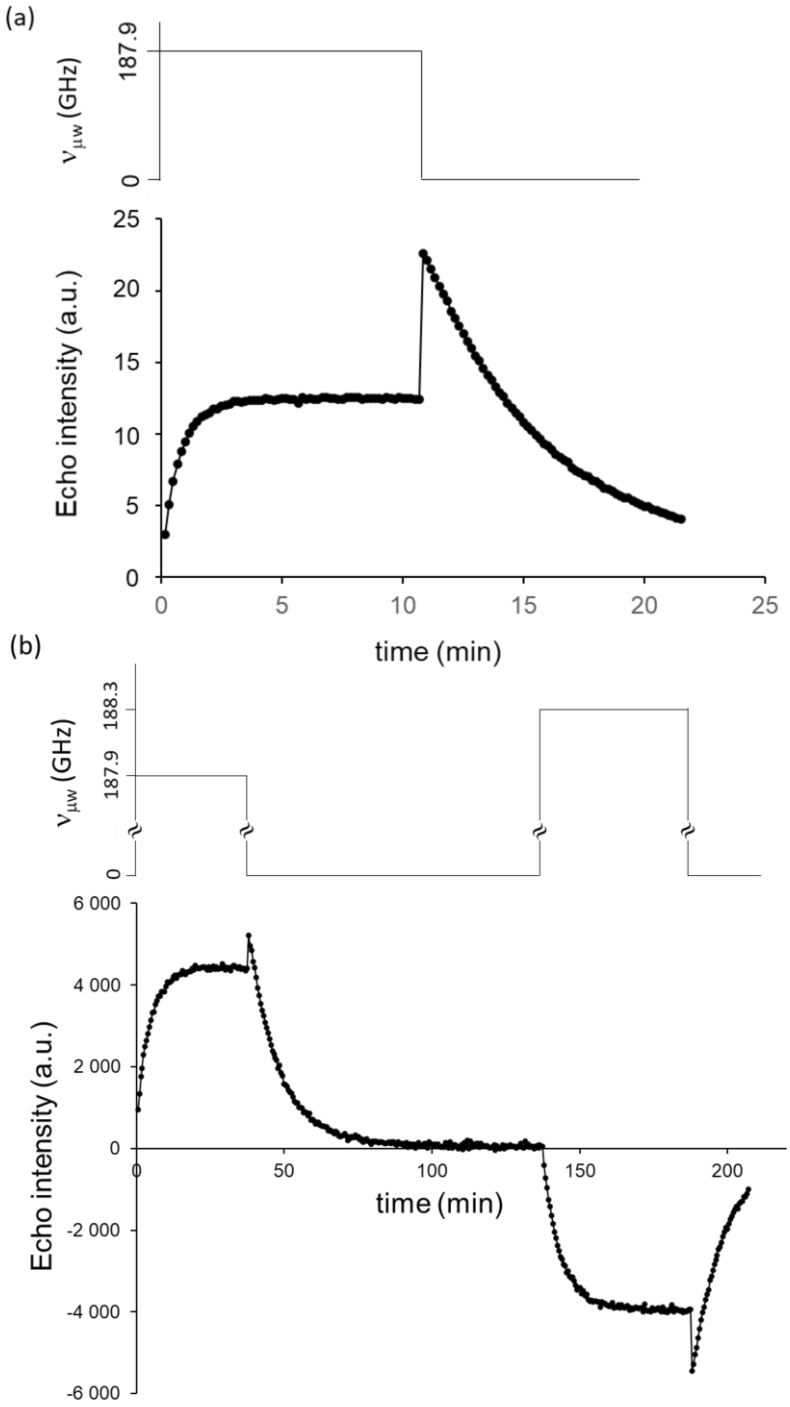

Figure 3 **(a)** Build-up curve of dipolar proton echoes of sample **III**. The data points were acquired at intervals of 30 s. Note that the time-scale of the surges is much shorter than in Fig. 1b. **(b)** Build-up curve for sample **IV**. The top panel indicates that the microwave irradiation was initially applied on the negative lobe of the EPR spectrum at 187.9 GHz, then switched off, and finally applied to the positive lobe of the EPR spectrum at 188.3 GHz.

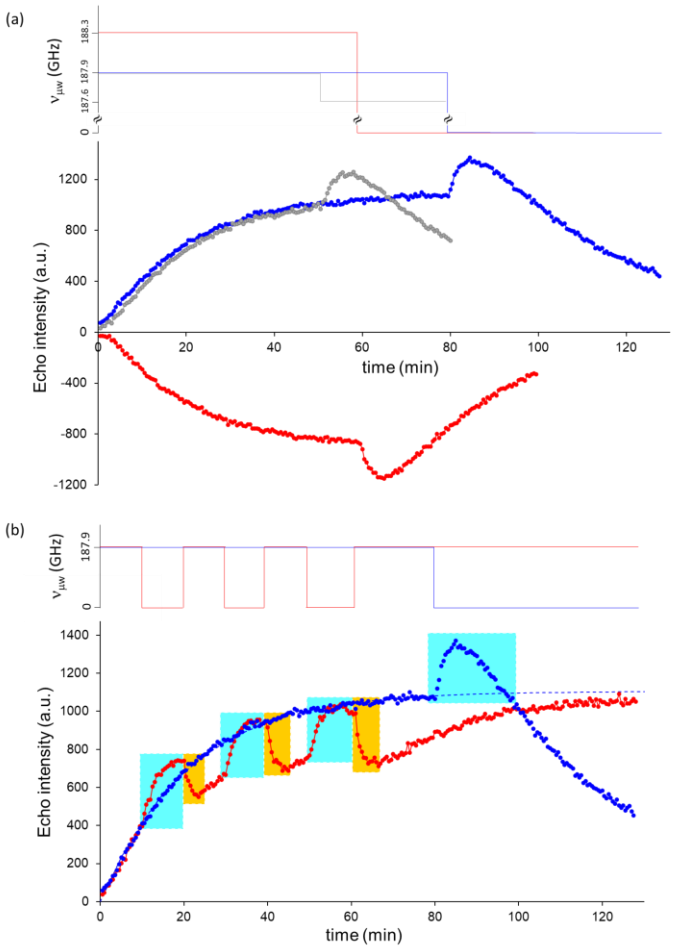

Figure 4 **(a)** Build-up curves of dipolar proton echoes of sample **V**, acquired at T_{sample} = 1.2 K in a static field B_0 = 6.7 T. Each data point results from the acquisition of a dipolar echo excited by means of a single β - τ_{echo} - β - τ_{echo} - sequence with β = 9°, τ_{echo} = 100 µs and an rf amplitude ν_1 = 50 kHz, without phase-cycling. The intervals between the points were 30 s in all cases. The transient surges of the polarization are highlighted by cyan rectangles. The top panel indicates the points in time where microwave irradiation is either switched off or shifted off-resonance. The blue points refer to experiments where microwave irradiation was initially applied at 187.9 GHz, i.e., on the negative lobe of the EPR spectrum. The grey points refer to an experiment where microwaves were not turned off but where their carrier frequency was shifted to 187.6 GHz, far off-resonance with respect to the EPR spectrum, showing that the surge is not due to a change in sample temperature associated with switching the microwave field. The red points refer to experiments where the microwave irradiation was applied to 188.3 GHz, on the positive lobe of the EPR spectrum. **(b)** Build-up curves of dipolar proton echoes of sample **V** analogous to those of Fig. 4a. The blue data points are the same as in Fig. 4a, shown for comparison. A mono-exponential fit of these points is shown by a dashed blue curve ($T_{build\text{-}up}$ = 21.0 ± 0.2 min). Red points relate to experiments where the microwave field was turned on and off at different points along the build-up of the signal, as indicated in the top panel. Transient surges and slumps of the echoes are highlighted by cyan and dark yellow rectangles. The final level of the hyperpolarization achieved under microwave irradiation is the same in both experiments, as indicated by the blue dashed curve. If the microwave field is not switched on again, the polarization decays under the combined effect of spin-lattice relaxation and saturation by *rf* pulses, because of the large number of pulses with small nutation angles.